iScience

Article

Contribution of neurons that express *fruitless* and *Clock* transcription factors to behavioral rhythms and courtship

Graphical abstract

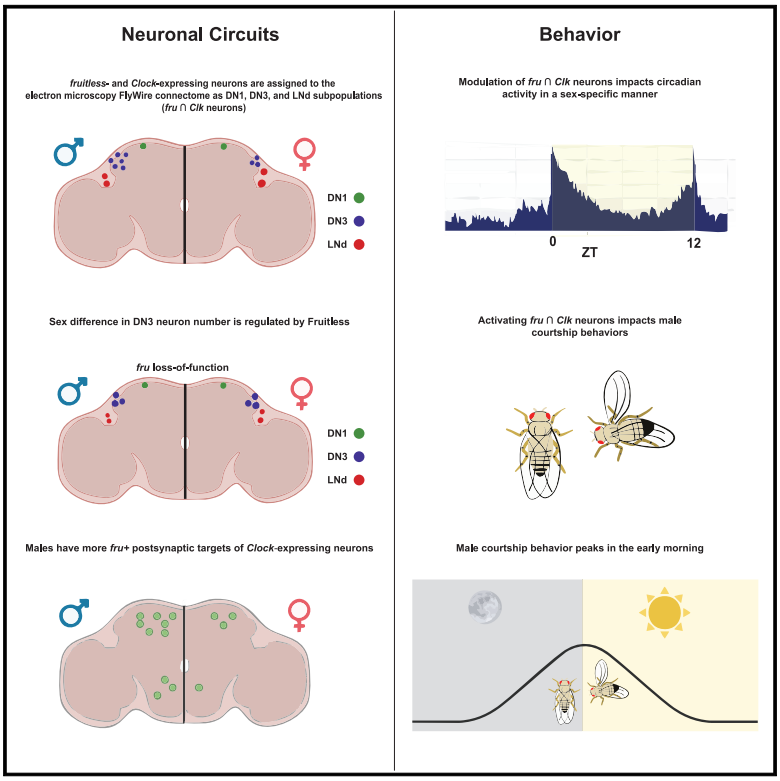

Highlights

- Assigned *fru* ∩ *Clk* neurons to FlyWire connectome as DN1, DN3, and LNd populations
- Higher number of DN3 *fru* ∩ *Clk* neurons in males is regulated by *fruitless*
- Males have more *fru* post-synaptic neurons downstream of core circadian neurons
- Modulation of *fru* ∩ *Clk* neuronal activity sex-specifically changes behavior

Authors

Anthony Deluca, Brooke Bascom, Daniela A. Key Planas, Matthew A. Kocher, Marielise Torres, Michelle N. Arbeitman

Correspondence

michelle.arbeitman@med.fsu.edu

In brief

Molecular biology; Neuroscience

Deluca et al., 2025, iScience *28*, 112037
March 21, 2025
https://doi.org/10.1016/j.isci.2025.112037

CellPress

iScience

CellPress
OPEN ACCESS

Article

Contribution of neurons that express *fruitless* and *Clock* transcription factors to behavioral rhythms and courtship

Anthony Deluca,[1,2] Brooke Bascom,[1,2] Daniela A. Key Planas,[1,2] Matthew A. Kocher,[1,2] Marielise Torres,[1] and Michelle N. Arbeitman[1,3,*]

[1]Department of Biomedical Sciences, College of Medicine, Florida State University, Tallahassee, FL 32306, USA
[2]These authors contributed equally
[3]Lead contact
*Correspondence: michelle.arbeitman@med.fsu.edu
https://doi.org/10.1016/j.isci.2025.112037

SUMMARY

Animals need to integrate information across neuronal networks that direct reproductive behaviors and circadian rhythms. The Drosophila master regulatory transcription factors that direct courtship and circadian rhythms are co-expressed. We find sex differences in the number of these *fruitless* (*fru*) and *Clock* (*Clk*)-expressing neurons (*fru* ∩ *Clk* neurons) regulated by male-specific Fru. We assign the *fru* ∩ *Clk* neurons to the electron microscopy connectome and to subtypes of clock neurons. We discover sex differences in *fru*-expressing neurons that are post-synaptic targets of *Clk*-expressing neurons. When *fru* ∩ *Clk* neurons are activated or silenced, we observe a male-specific shortening of period length. Activation of *fru* ∩ *Clk* neurons also changes the rate a courtship behavior is performed. We examine male courtship behavior over 24 h and find courtship activities peak at lights-on. These results reveal how neurons that subserve the two processes can impact behavioral outcomes in a sex-specific manner.

INTRODUCTION

Reproductive behaviors and circadian rhythms are biologically linked. For example, the time-of-day influences when animals mate, and reproductive behaviors and mating in turn impact daily activity patterns and sleep. In *Drosophila melanogaster*, the neuronal networks that direct reproduction and circadian rhythms are largely distinct, but there are neurons predicted to function in, or link, both processes, given that they express the master regulatory transcription factors that underlie both reproduction and daily rhythms. A set of transcription factors encoded by *period (per)*, *timeless (tim)*, *Clock (Clk)*, and *Cycle* (*Cyc*) are part of a regulatory feedback loop to direct circadian rhythms.[1] The sex determination hierarchy gene *fruitless* encodes sex-specific transcription factors that are produced in neurons that underlie male and female reproductive behaviors.[2] In our previous single-cell RNA-sequencing study, directed at molecularly classifying the repertoires of *fruitless*-expressing neurons that direct reproductive behaviors,[3] we identified a set of neurons in both sexes that also express the master clock genes (*fru* ∩ *Clk* neurons). Here, we examine the role of *fru* ∩ *Clk* neurons in generating sex differences in behavioral rhythms and determine if there are additional functions for reproductive behaviors.

The network of neurons directing circadian rhythms is composed of ~150 neurons in the brain that have been ascribed different functions. These neurons are named for their neuroanatomical positions. The *fru* ∩ *Clk* neurons are defined by molecular genetic tools and include a subset of each of the following classes of clock neurons: LNds (dorsal-lateral neurons), DN1s (dorsal), and DN3s (dorsal) clock neurons. The LNds direct evening anticipation in light:dark conditions (LD) and are part of the set of "evening" or "E" cells. The DN1s are targets of the sLNv "morning" or "M" neurons. The sLNvs are pacemaker neurons that are critical for behavioral activity rhythms and produce pigment dispersing factor (PDF), a neuropeptide that keeps the clock neuronal network synchronized. The DN1s have been ascribed several functions, including activity promoting,[4] sleep promoting,[5,6] and coordinating the response to light and temperature.[7] The DN3s are not as well studied, though do have a role in promoting sleep.[8]

The potential for Drosophila reproductive behaviors is specified by the sex determination hierarchy.[9] This hierarchy is composed of a pre-mRNA splicing cascade that is a readout of the number of X chromosomes. At the bottom of the hierarchy are two genes that encode transcription factors that have pre-mRNAs that are spliced in a sex-specific manner. These transcription factors control all aspects of sexual differentiation in non-germline tissues (*doublesex* [*dsx*] and *fruitless* [*fru*]). Both *dsx* and *fru* direct reproductive behaviors through production of sex-specific transcription factors, with *fru* being expressed in a larger population of neurons. *dsx* also directs all aspects of somatic sexual differentiation outside of the nervous system. The *fru* transcripts produced from the *fru P1*

promoter are the sex-specifically spliced *fru* transcript class, that produces male-specific transcription factors (Fru^M). It is thought that no functional female-specific Fru product is produced. *fru P1*-expressing neurons are found in both sexes and have similar neuroanatomical positions and numbers.[10,11] These *fru P1* neurons underlie reproductive behaviors in both sexes, based on several types of molecular-genetic perturbation studies.[12]

Here, we examine *fru* ∩ *Clk* neurons that are molecularly defined using a genetic intersectional approach that relies on *fru P1* regulatory elements driving expression of *flippase* (*fru-Flp*),[13] the *Clk856-Gal4* transgene (*Clk-Gal4*) that drives expression in the core clock neurons of UAS-controlled transgenes,[14] and a set of *UAS-Flp-out* cassette transgenes that have expression limited to neurons with overlapping *fru-Flp* and *Clk-Gal4* expression. We extend our neuroanatomical examination of sex differences in these neurons using a MultiColor FlpOut (MCFO) stochastic labeling approach, coupled with links to the Drosophila FlyWire connectome that is based on serial electron micrographic studies. We further characterize *fru* neurons in the core clock using the same genetic intersectional strategy with *fru-Flp* and *Gal4* transgenes for a set of genes with known core clock expression. Furthermore, we identify sex differences in the number of *fru P1* neurons that are targets of the core clock neural network, using a *trans*-synaptic labeling approach (*trans*-Tango).[15] We found that either activating or silencing the *fru* ∩ *Clk* neurons results in a shorter circadian period and more activity in constant dark conditions (DD), but only in males. Activation and silencing of *fru* ∩ *Clk* neurons had modest impacts on overall activity in LD conditions. We found that the changes in behavioral rhythmicity were reflected in Per cycling in the sLNvs neurons, when *fru* ∩ *Clk* neurons were either activated or silenced. Male courtship behavior was impacted by *fru* ∩ *Clk* neurons activation, with more attempts to copulate per minute observed, linking the *fru*-expressing circadian neurons to reproductive activity. We examine courtship across a 24-h window and find that males have peak courtship activity at lights-on, with increases observed in anticipation of lights-on starting ~2 h prior. The *fru* ∩ *Clk* neuron perturbations did not significantly impact the timing of courtship across the 24-h window we examined. Taken together, we have found links between sex-specific circadian governance of daily activity and reproductive outputs.

RESULTS

Characterization of *fru* ∩ *Clk* neurons

To visualize neurons that express both *fru P1* (hereafter *fru*) and *Clk* (*fru* ∩ *Clk*), we employed a labeling approach called MultiColor FlpOut (MCFO) that relies on expression of both *fru-Flp* and *Clk-Gal4* for the visualization of individual neurons and their projections in different colors, using confocal microscopy (Figure 1A; Video S1; called *fru* ∩ *Clk* MCFO neurons).[13,14,16] We first observed *fru* ∩ *Clk* MCFO neurons over a 24-h period, in animals that are aged 5–10 days old, across six time points, to determine if there were large changes in neuronal projection patterns influenced by the time of day, as observed for sLNvs.[17] We did not observe any large changes across the six time points (Figure S1), though further higher resolution analyses may reveal small differences. We did an in-depth characterization of the full set of *fru* ∩ *Clk* MCFO neurons from animals at zeitgeber time (ZT) 4–6, as this overlaps with the time we perform courtship analyses. We observe expression in a subset of the DN1s, DN3s, and LNds, as before,[3] with projections within the protocerebral region for the DN1s and DN3s, including some with projections that cross the midline. Additionally, our labeling identifies neurons in the subesophageal zone (SEZ), ascending median bundle neurons, and in the ventral nerve cord (VNC), with most in the abdominal ganglion of the VNC. We also visualize the *fru* ∩ *Clk* neurons using an additional Flp-out responsive cassette (*UAS <stop <smGDP::myc* on the second chromosome; smGDP tool) to determine if the triple MCFO is a reliable tool to visualize neurons (Figure S2). We find that the triple MCFO reporter detects more *fru* ∩ *Clk* neurons than the smGDP tool, so we proceeded with our analyses using MCFO.

To further characterize *fru* neurons in the clock, we determined the intersection with other genes in the core clock (*cryptochrome*: *fru* ∩ *cry* and *timeless fru* ∩ *tim*; Figures S3–S5).[19,20] We find overlap consistent with *Clk856-Gal4* and additional intersecting neurons that were not previously detected (Figure S4). We also examined the overlap of *fru* with Gal4 transgenes that are inserted into neuropeptide genes that are known to be expressed in the core clock neurons, as previously described.[18,21,22] We find *fru* ∩ *AstC* and *fru* ∩ *AstC split-Gal4* have expression in the DN3 region, consistent with previous findings on circadian roles of *AstC*[23,24] (Figure S3), whereas other *fru* ∩ *neuropeptide Gal4* transgene combinations did not have overlapping expression that is similar in morphology to *fru* ∩ *Clk* neurons (Figure S5). Future behavioral studies on these different *fru* ∩ core clock gene subsets will shed light on the roles of additional neuronal subsets.

FlyWire connectome classification of *fru* ∩ *Clk* brain neurons

Given our higher resolution morphological analyses of the *fru* ∩ *Clk* neurons with MCFO, we are able to classify them using the FlyWire connectome database, a circadian network connectome based on FlyWire, and annotation of *fru*+ neurons in the FlyWire connectome.[18,25,26] All the connectome neurons shown in Figure 1 are labeled as *fru*+, except the DN1pAs, providing further confidence in our assignments. The circadian connectome lists five types of DN3s. The *fru* ∩ *Clk* DN3s are likely DN3c (s-$CPDN_3C$),[18] and/or DN3d (s-$CPDN_3D$),[18] given they have projections in the protocerebral region, with some crossing the midline over the pars intercerebralis (PI). This is not observed for s-$CPDN_3B$ and s-$CPDN_3E$ neurons. We also rule out s-$CPDN_3A$ neurons because these have projections into the optic lobe, which we do not observe. For DN1s, we found the DN1pA neurons were most similar to *fru* ∩ *Clk* DN1 neurons. There was another classified set of DN1 neurons that have projections above the DN1 region that we did not observe in our MCFO staining. We propose the *fru* ∩ *Clk* LNds are LNdb and LNdc and not the third category called LNda. The LNda have a large projection into the optic lobe that we did not observe. Using the FlyWire resource, we generated a composite of the neuronal

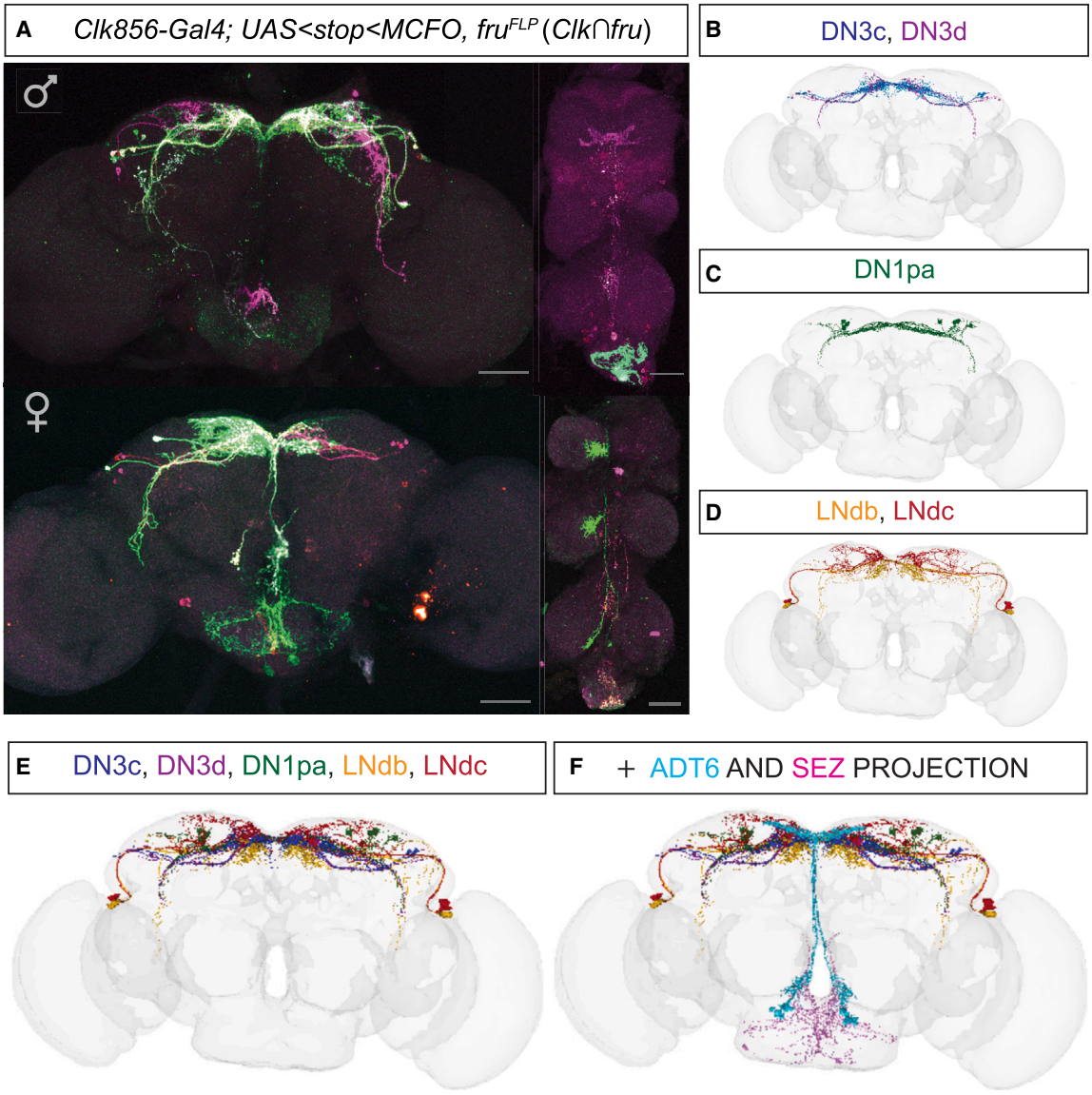

Figure 1. FlyWire connectome classification of *fru* ∩ *Clk* brain neurons

(A) Brain and VNC confocal maximum projections from 5- to 10-day-old adults. *fru* ∩ *Clk* neurons are identified using the MultiColor FlpOut (MCFO; *UAS <Stop <MCFO*) reporters. Scale bars, 50 μm. Images were acquired with a 20X objective. The genotype is *w, Clk856-Gal4/+; UAS <Stop <MCFO, fru^{FLP}/+*. The epitopes detected in MCFO staining are HA, Flag, and V5.

(B–D) FlyWire 3D projections of s-CPDN$_3$C (DN3c), s-CPDN$_3$D (DN3d), DN$_{1p}$A (DN1pa), LN$_d$B, and LN$_d$C (LNdb and LNdc) neurons. The nomenclature is from the published circadian connectome.[18]

(E) Combined FlyWire projections of DN3c, DN3d, DN1pa, LNdb, and LNdc neurons.

(F) Addition of FlyWire ADT6 and SEZ projections with DN3c, DN3d, DN1pa, LNdb, and LNdc neurons.

classes (DN3c, DN3d, DN1pa, LNdb, and LNdc) that is similar to the *fru* ∩ *Clk* MCFO pattern (Figure 1E).

Although neurons in the SEZ are not part of the defined ~150 clock network, we identify them in the *fru* ∩ *Clk* MCFO staining. We observe median bundle neurons that project from the SEZ to the PI region that are similar in morphology to ADT6 neurons *(fru$^+$)*, though we note that there are over 230 ADT6 neurons that are difficult to distinguish by morphology. The cb1008 ADT6 neurons have similar cell numbers and projection. The cb1008 neurons also had projections near the DN3 and DN1 neurons, as we see in *fru* ∩ *Clk* MCFO staining, which gave us higher confidence. The projections we see in the SEZ were variable; however, the overall cell body positioning and ring shape of the neurites is similar to an unlabeled neuron notated as cb0456 in FlyWire. Using the FlyWire resource, we generated a composite of all the potential neuronal classes that is highly similar to the *fru* ∩ *Clk* MCFO pattern (Figure 1F).

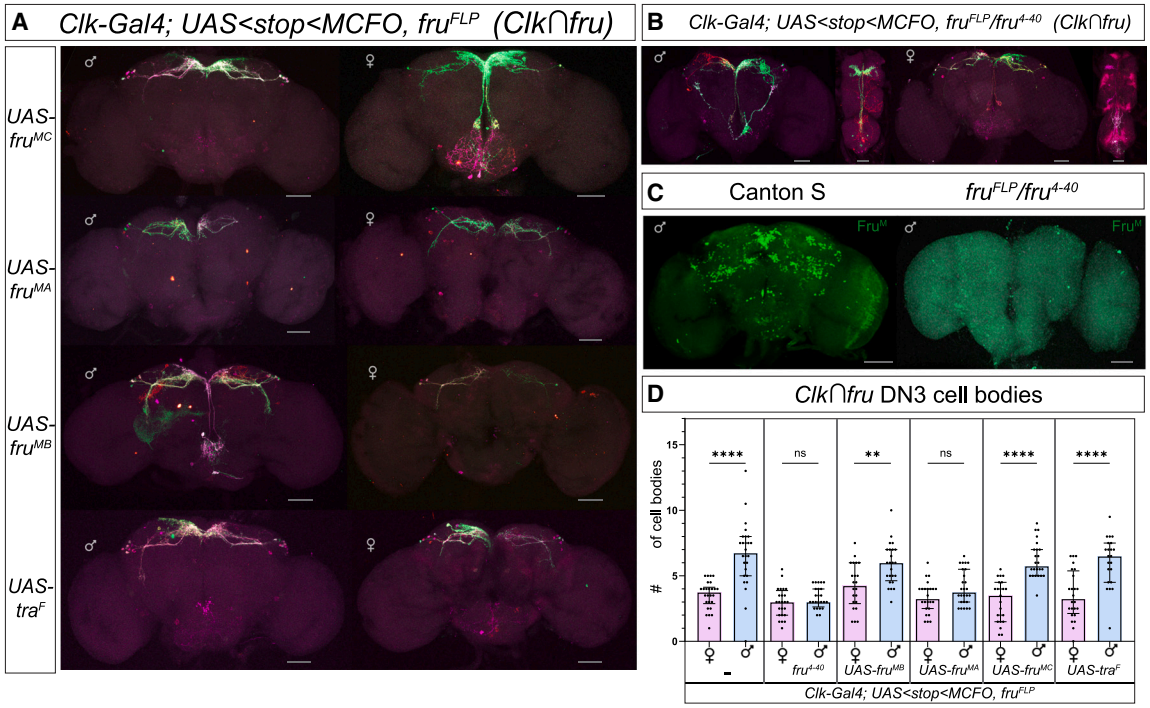

Figure 2. Impact of the sex hierarchy on *fru* ∩ *Clk* neuron number

(A and B) Brain and VNC confocal maximum projections from 5- to 10-day-old adults. The genotype is: *w, Clk856-Gal4/+; UAS <Stop <MCFO, fru^{FLP}/+*. Images show *fru* ∩ *Clk* neurons identified using the MultiColor FlpOut (MCFO) reporters. (A) MCFO staining with overexpression of Fru^{M} isoforms (Fru^{MA}, Fru^{MB}, or Fru^{MC}) or Tra^{F} under UAS regulation. The genotype includes one of the UAS transgenes on the second chromosome. (B) MCFO staining in *trans*-heterozygous *fru* allele combination *fru^{FLP}/fru$^{4–40}$*.

(C) Brain confocal maximum projections from 5- to 10-day-old adults. Wild-type (Canton S strain) and *fru^{FLP}/fru$^{4–40}$* brains were stained with anti-Fru^{M} antibody.

(D) Count of DN3 neurons in males and females at the ZT4-6 time window. Bar graphs show median with interquartile range. Two-tailed Mann-Whitney test comparing males and females for each effector. *$p < 0.05$, **$p < 0.01$, ***$p < 0.001$, ****$p < 0.0001$. $n = 22–26$ hemibrains for each genotype examined, for both males and females. Scale bars, 50 μm. Images were acquired with a 20X objective.

Impact of the sex hierarchy on *fru* ∩ *Clk* neuron number

The *fru* ∩ *Clk* MCFO staining revealed that males had more DN3 neurons, compared to females. Scoring the number of *fru* ∩ *Clk* brain DN3 neurons blinded showed that males have ~6.75 and females have ~3.75 (median counts; Figures 2A–2D). To determine if these differences are regulated by *fru*, we examined the number of *fru* ∩ *Clk* DN3 neurons when we overexpress different Fru^{M} isoforms that differ in their DNA-binding domain (Fru^{MA}, Fru^{MB}, or Fru^{MC}). *fru* is a complex locus, with at least five potential alternative 3′ exons that encode DNA binding domains,[27] with the A, B, and C encoding exons being the predominant ones in the nervous system. These male-specific Fru isoforms bind different DNA elements and have different target genes and different functions.[28–30] Overexpression of Fru^{MB} lead to an increase in *fru* ∩ *Clk* DN3 female neurons compared to no overexpression, though genotype-matched males still had significantly more. Overexpression of Fru^{MA} leads to a decrease in *fru* ∩ *Clk* DN3 male neurons, resulting in no significant difference in neuron number between the sexes in that comparison (Figure 2D). Overexpression of Fru^{M} isoforms also impacted whether different sets of *fru* ∩ *Clk* MCFO neurons were detected in a brain (Figure S6), with each isoform having unique phenotypes. These results are consistent with known differences in functions of the Fru^{M} isoforms.[28–30]

When we examine a strong hypomorphic, *trans*-heterozygous *fru* allele combination that substantially reduces the amount of Fru^{M} protein (*fru$^{4–40}$/fru^{FLP}*; Figure 2C),[31] we find the number of *fru* ∩ *Clk* DN3 male neurons is reduced to the same number as female (Figure 2D). We do not see this same result when we feminized the neurons by expressing Tra^{F}, which is predicted to remove Fru^{M} from all neurons that express *Clk-Gal4*. The difference in the results may be because *fru$^{4–40}$/fru^{FLP}* results in a loss of Fru^{M} at any time Fru^{M} is produced, whereas the UAS-transgene manipulations are under the control of *Clk* expression, which may be at a later developmental time. Additionally, there could be a cell-nonautonomous requirement for *fru* for male *fru* ∩ *Clk* DN3 neurons. Across all these molecular-genetic manipulations changes were observed in the percentage of animals with a structure, or the number of neurons present, though we did not see large changes in projection patterns, consistent with the observation that we did not see obvious morphological sexual dimorphism in *fru* ∩ *Clk* MCFO neurons.

fru post-synaptic targets of circadian network neurons are dimorphic

To determine if there is additional sexual dimorphism in the circadian neural network, we identified the *fru* synaptic targets

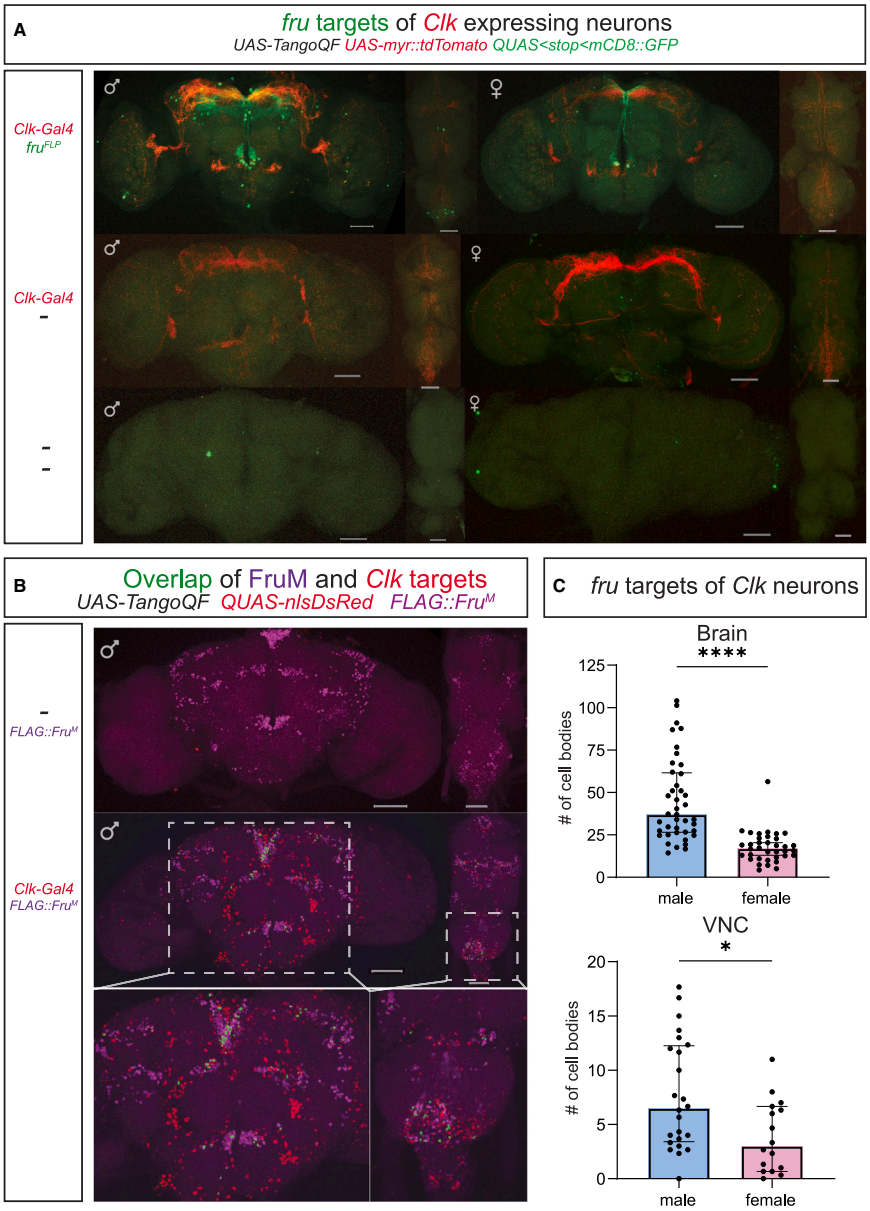

Figure 3. *fru* post-synaptic targets of circadian network neurons are dimorphic

(A) Brain and VNC confocal maximum projections from 5- to 10-day-old male and females adults. The *trans*-Tango reporter tool allows for visualization of *Clk856-Gal4* neurons (red) and *fru* synaptic targets of *Clk* (green). The genotype contains these elements: *trans-Tango/Clk856-Gal4; 10XUAS-IVS-myr::tdTomato, QUAS <stop <mCD8-GFP/fru^{FLP}*. The QF transcription factor is produced in the post-synaptic targets of *Clk*, with the QF-dependent reporter, *QUAS*, only active in *fru* neurons. Scale bars, 50 μm.

(B) Brain and VNC confocal maximum projections from 5- to 10-day-old adults. The *trans*-Tango reporter tool allows for visualization of targets of *Clk856-Gal4* neurons (nuclear dsRed). These flies harbor a Crispr-modified *fru* allele that generates an amino-terminal Flag-tagged Fru^{M} (Flag::Fru^{M}; anti-Flag purple). The genotype contains these elements: *5XQUAS-nlsDsRed; trans-Tango/Clk856-Gal4;Flag::Fru^{M}*. Colocalization of the red and purple signal is shown in green. Scale bars, 50 μm.

(C) Male and female cell body counts of the post-synaptic *fru* targets of *Clk* neurons from (A), per brain, and VNC. Bar graphs show median with interquartile range (IQR) and two-tailed Mann-Whitney test. Male brain: $n = 41$ brains, IQR = 25–57, range = 13–115; female brain: $n = 36$, IQR = 11–19, range = 3–55; male VNC: $n = 24$, IQR = 3.25–12, range = 0–17; female VNC: $n = 16$, IQR = 1–6.75, range = 0–11. $^{*}p < 0.05$, $^{****}p < 0.0001$.

of *Clk-Gal4* neurons, using the *trans*-Tango reporter system (Figure 3).[15] First, we restrict the *trans*-Tango post-synaptic reporter to *fru* neurons, by using a reporter that relies on expression of *fru^{FLP}* (green; Figure 3A). We observe sex differences in the number and position of the *fru* synaptic targets, with more neurons in the male brain (Figures 3A and 3C). These *fru* synaptic targets are neurons in the posterior region of the brain with cell bodies near where the mushroom body cell bodies reside (here called midbrain cloud), ascending median bundle, and arch and lateral junction of the lateral protocerebral complex. If we examine individual brain regions, we find males more often have the midbrain cloud and the arch neurons detected (Figure S7), whereas in females we more often detect the ascending median bundle neurons (Figure S7). We also detect more neurons in the ventral nerve cord (VNC) in males (Figure 3C), in the VNC abdominal ganglion and VNC T2 midline neurons (Figure 3A). We also examined *fru* synaptic targets of *Clk-gal4* using a reporter for all *Clk-gal4* post-synaptic targets (Figure 3B; nuclear red) and detected their overlap with Fru^{M} (Figure 3B; nuclear purple Fru^{M} tagged with FLAG epitope, and green shows overlap). This approach revealed additional *fru* post-synaptic *Clk*-target neurons with cell bodies in the PI, though overall was consistent with the results using the *trans*-Tango FLP-out reporter approach.

fru ∩ *Clk* neuronal activity impacts circadian period

Next, we determine the function of *fru* ∩ *Clk* neurons in circadian period length, by either activating (*UAS < stop<TrpA1;* hereafter called *TrpA1*) or silencing (*UAS < stop<Kir2.1*; hereafter called *Kir2.1*) *fru* ∩ *Clk* neurons (Figure 4; Table S1), in strain-background-matched conditions. Similar to our previous study,[3] in constant dark conditions, we found activating *fru* ∩ *Clk* neurons resulted in males having a significantly shortened period length (23.2 h) compared to controls, but females were similar to controls (23.8 h for females), though they had a lower percentage of rhythmic flies. We were surprised that silencing

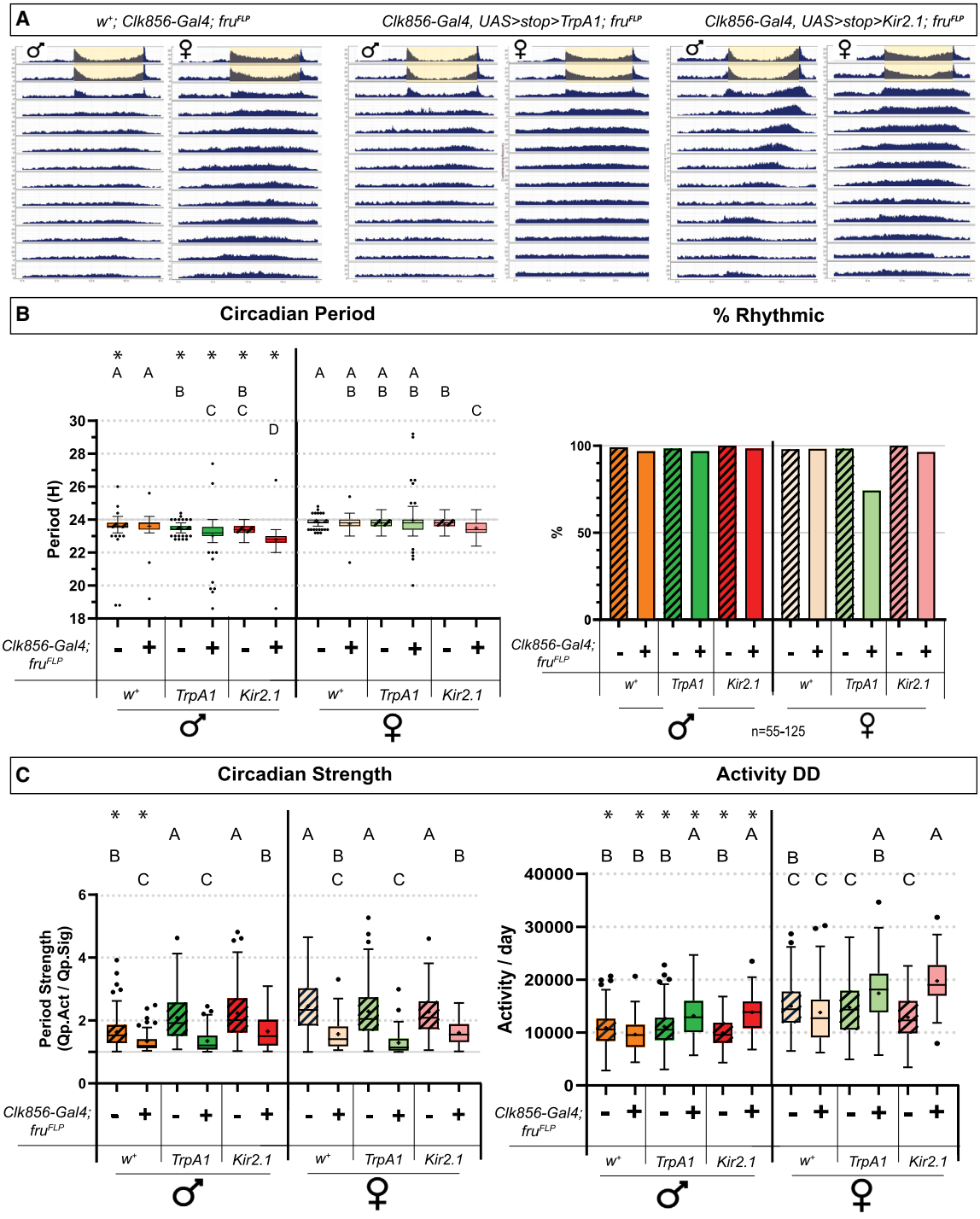

Figure 4. *fru* ∩ *Clk* neuron activity impacts circadian period and overall activity

(A) Actograms showing averaged activity over 2 days in light dark and 11 days in constant dark. The yellow shaded region indicates when lights are on at the end of light:dark entrainment (first 2 days in monitors). Males and females are (1) w^+, *Clk856-Gal4/+; fru*^{FLP} (controls, male $n = 62$, female $n = 59$), (2) *w; Clk856-Gal4/UAS <stop <TrpA1; fru*^{FLP}/+. (TrpA1 activated, male $n = 62$ female $n = 62$), and (3) *w; Clk856-Gal4/UAS <stop <Kir2.1; fru*^{FLP}/+. (Kir2.1 silenced, male $n = 62$ female $n = 55$). Y axis range 0–35 counts. X axis is a 24-h time period. The data are plotted in 5-min bins.

(B) Circadian period and % rhythmic flies.

(C) Circadian strength reported as Qp.act/Qp.sig. and average activity per day (right) were calculated using ShinyR-DAM.[32]

(legend continued on next page)

fru ∩ *Clk* neurons also significantly reduced circadian period in males (22.8 h) and females (23.4 h), compared to controls (Figures 4A and 4B; Table S1). Experimental males and females did not differ from controls for circadian strength, with the presence of only the *Clk-Gal4* and *Fru-Flp* transgenes also causing a reduction in circadian strength (Figure 4C). Animals with either silenced (*Kir2.1*; males and females) or activated (*TrpA1*; males and females) *fru* ∩ *Clk* neurons had more overall activity compared to same-sex, strain-matched controls (w^+), which could be related to the shortened circadian period in males. The observation that continuous activation or silencing of *fru* ∩ *Clk* neurons had the same shortened circadian period phenotype in males is consistent with a need for *fru* ∩ *Clk* neurons to change their activity across the day and night to maintain wild-type period.

To further determine if the sex-specific identity of *fru* ∩ *Clk* neurons impacted the sex-specific phenotypes we observed when *fru* ∩ *Clk* neurons are either activated or silenced, we introduced transgenes that either feminize (*UAS-Tra*^{F}) or masculinize (*UAS-tra* and *UAS-tra-2* RNAi) neurons and did not see an impact on the sex difference of the circadian phenotype (Table S1). This could be due to the timing of transgene expression, as the RNAi and overexpressors may be turned on later then when sex identity is established. In addition, we show that the male-specific reduced circadian phenotype is due to *fru* ∩ *Clk* neurons in the brain, by introducing a transgene that blocks *Clk-Gal4* activity in the VNC (*tsh-Gal80*), though we note that the *tsh-Gal80* transgenes made the flies less healthy overall (Figure S8).[33]

When we filtered the data to require that flies have a stronger period strength (strength >1.1; Figure S9), we found a similar shorter circadian period phenotype in males, when *fru* ∩ *Clk* neurons are activated and silenced. From this analysis it is clear that activating *fru* ∩ *Clk* neurons causes arrhythmicity in both males and females (Figure S9).

Period cycling is shifted due to changes in *fru* ∩ *Clk* neuron activity

Next, to understand how the shortened circadian period arises when *fru* ∩ *Clk* neuron activity is altered, we examined Per cycling in the critical sLNvs clock pacemaker neurons. Per protein immunostaining across six time points, starting 7 days after the initiation of constant dark conditions, reveals a similar phase shift when *fru* ∩ *Clk* neurons are either activated or silenced, consistent with the change in behavior (Figure S9), as compared to Canton S and *Clk-Gal4, Fru-Flp* controls. We expect to observe a ∼7- to 8-h shift in per cycling after 7–8 days in DD. The *fru* ∩ *Clk* neurons (DN1, DN3, and LNds) are thought to be downstream of the sLNv pacemaker neurons. This suggests that there may be feedback to the sLNvs either through synaptic connections, or indirectly, via the changes in behavior that are directed by *fru* ∩ *Clk* neurons. It has been shown that sLNvs are a target of DN1 neurons and that DN1 neurons have robust sex differences in activity.[5] Our results may provide further evidence that *fru* ∩ *Clk* neurons feedback on the core pacemaker sLNvs to change rhythmic behaviors.

Impact of *fru* ∩ *Clk* neuron number and sex-specific identity on circadian period

Given the fru^{4-40}/fru^{FLP} genetic background resulted in a loss of sexual dimorphism in *fru* ∩ *Clk* DN3 neuron number (Figure 2), we wanted to determine if the sex difference in DN3 neuron number is responsible for the male-specific reduction in circadian period length with activated or silenced *fru* ∩ *Clk* neurons (Figure 4). To better understand the fru^{4-40}/fru^{FLP} *trans*-heterozygous allele combination, we tested males in courtship assays. Across all metrics, fru^{4-40}/fru^{FLP} *trans*-heterozygotes had reduced courtship activity as compared to wild-type males, though they still courted (Figure S10). This indicates that the fru^{FLP} allele is a partial loss of function, despite the lack of Fru^M staining we observed in fru^{4-40}/fru^{FLP} (Figure 2), as previously suggested.[34] Unexpectedly, the fru^{4-40}/fru^{FLP} males and females both show a reduced circadian period when *fru* ∩ *Clk* neurons are activated or silenced, indicating that the large fru^{4-40} deficiency or genetic background has a non-sex-specific genetic interaction causing a reduced circadian period (Figure S10). Therefore, it is not clear if the reasons males show a reduced circadian period when *fru* ∩ *Clk* neurons are either activated or silenced is due to differences in DN3 neuron number.

fru ∩ *Clk* neuronal activity impacts activity

We also examined activity when *fru* ∩ *Clk* neurons are either activated (*TrpA1*) or silenced (*Kir2.1*), in 12-h light and 12-h dark conditions (LD), using strain-background-matched conditions (Figure S11). When *fru* ∩ *Clk* neurons are activated (*TrpA1*), males have increased LD activity (left panel), whereas the male controls all have similar activity (right panel). This appears to be due to an increase of nighttime activity in males when *fru* ∩ *Clk* neurons are activated (*TrpA1*) (Figure S11). Across all genotypes, males are less active than females, in total daily activity, except when males *fru* ∩ *Clk* neurons are activated (Figure S11). To determine if there are structural differences in activity in LD, we examined averaged activity data across day and night. Males of all three genotypes show a rapid reduction in activity after lights-on (ZT 0), compared to females, and a longer afternoon siesta, as previously reported.[1] One trend in the data is that males (red; Figure S11) and females (pink; Figure S11) with *fru* ∩ *Clk* neurons silenced *(Kir2.1)* reduced their activity more quickly after lights-on. Consistent with our observation that males with activated *fru* ∩ *Clk* neurons (*TrpA1*) have increased nighttime activity, these males show a much larger peak in activity after lights-off (dark green; ZT12; Figure S11) and continue to remain more active during the night.

(A–C) All flies are strain matched. All boxplots are Tukey boxplots that include the data from rhythmic flies. The letters above the boxplot indicate significant differences within sex (Kruskal-Wallis with Dunn's multiple comparisons). If two groups share a letter, this indicates that the p value for the pairwise comparison between them was not smaller than 0.05. The asterisk above the male data indicates within genotype significant differences between the sexes (Mann-Whitney two-tailed U test; $p < 0.01$). See Table S1 for n. Three flies were removed in total that had activity above 60,000 counts (B and C). All data presented here were collected using DAM5H monitors (15 beam).

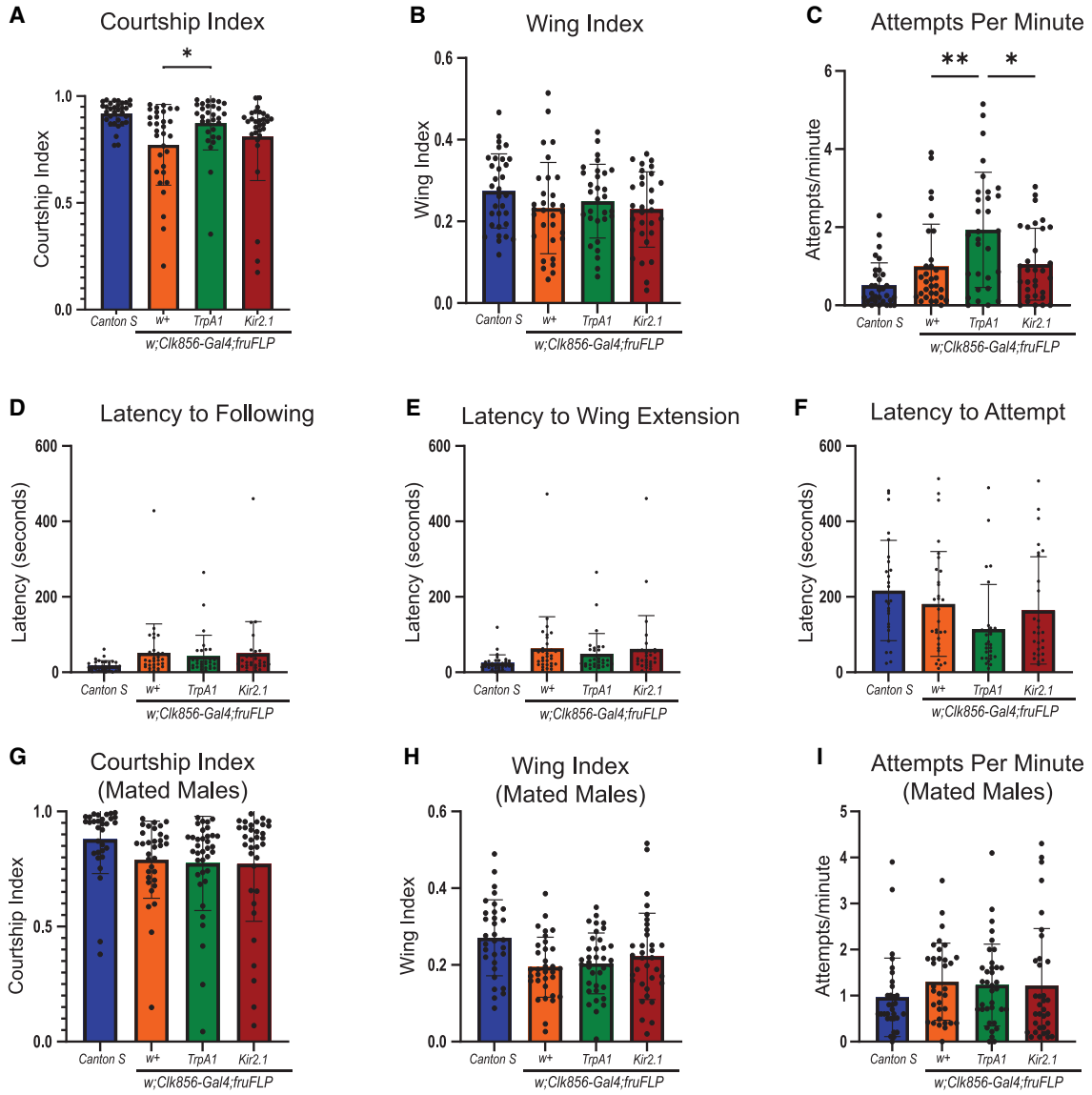

Figure 5. *fru* ∩ *Clk* neuronal activity has impacts on reproductive behavior

(A–F) Analysis of male courtship when *fru* ∩ *Clk* neuronal activity is altered. Courtship data show mean ± SD, with Kruskal-Wallis with Dunn's multiple comparisons for statistical test, unless otherwise indicated. $n = 30–32$ per genotype. (A) Courtship index measured as the time spent following divided by the total observation time. (B) Wing index measured as the time spent wing extending divided by the total observation time. One-way ANOVA with Tukey's multiple comparisons for statistical test. (C) Number of attempts per minute of observation time. One-way ANOVA with Tukey's multiple comparisons for statistical test. (D) Latency to following in seconds. (E) Latency to wing extension in seconds. (F) Latency to attempt in seconds. Flies that do not attempt are not included in the analysis.

(G–I) Courtship indices of males that were placed in the courtship assay following an initial mating. $n = 31–34$. Kruskal Wallis with Dunn's multiple comparisons for statistical analysis. (G) Courtship index (H) Wing extension index. (I) Attempts per minute. For all analyses, $^{*}p < 0.05$, $^{**}p < 0.01$, $^{***}p < 0.001$, $^{****}p < 0.0001$. The genotypes are w^{+}, *Clk856-Gal4/+;* fru^{FLP}/+ (controls), 2) *w; Clk856-Gal4/UAS <stop <TrpA1;* fru^{FLP}/+. (TrpA1 activated), and 3) *w; Clk856-Gal4/UAS <stop <Kir2.1;* fru^{FLP}/+. (Kir2.1 silenced).

fru ∩ *Clk* neuronal activity impacts reproductive behavior

To determine the role of *fru* ∩ *Clk* neurons in courtship, we examined courtship behavior when these neurons are either activated or silenced. Although the TrpA1 channel is temperature gated, all the circadian phenotypes we observed were in 25°C conditions. It is also known that the TrpA1 channel has temperature-independent activation.[35] For consistent comparisons, we test for courtship changes in the same conditions we saw circadian phenotypes. We saw a significant increase in overall courtship when the neurons are activated (courtship index; *TrpA1*) (Figure 5A) and an increase in the number of copulation

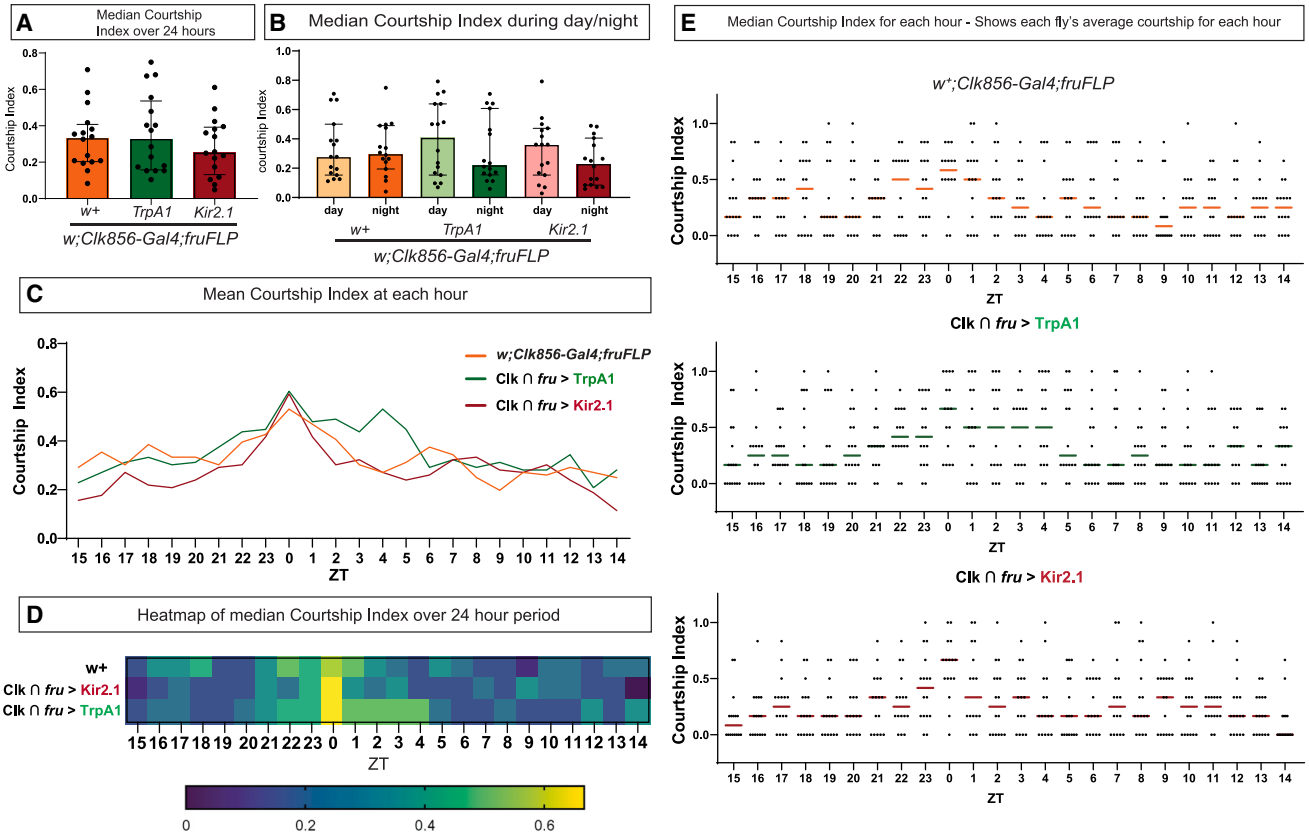

Figure 6. Circadian control of courtship across a 24-h period

(A) Courtship index (CI) over 24 h (n = 16 for each genotype).

(B) Courtship index over 12 h: data in (A) separated into day (12-h light) and night (12-h dark). (A and B) Each dot represents the % of time spent courting over a 24-h period (A) or 12-h period (B) for an individual fly. Graph shows median with interquartile range.

(C) Line graph showing the average CI. The average courtship of all 16 flies at each hour is shown. The x axis numbers indicate the ZT at the beginning of the hour.

(D) Heatmap showing median CI.

(E) The 16 dots show each fly's CI per hour. The colored dark line shows the median CI for all 16 flies. The genotypes are the same as in Figure 5.

attempts/per minute (Figure 5C), suggesting that *fru* ∩ *Clk* neurons have a role in courtship timing or gating (Figures 5 and S12).

To determine if mating status would reveal additional roles for *fru* ∩ *Clk* neurons, we examined courtship, mating, activity, and sleep in males and females after mating. Post-mating, males and females did not have differences in courtship and remating metrics, time to next mating, or sleep when *fru* ∩ *Clk* neurons are either activated or silenced (Figure S13). Across all genotypes, mated females show a decrease in sleep at night, compared to unmated controls, which is not impacted by activating or silencing *fru* ∩ *Clk* neurons. Activating or silencing the *fru* ∩ *Clk* neurons did not reveal post-mating differences in sleep compared to control *(w^+)* (Figure S13), though mated females with silenced *fru* ∩ *Clk* neurons *(Kir2.1)* had less overall activity compared to mated controls *(w^+)* (Figure S12). Therefore, *fru* ∩ *Clk* neurons do not appear to be important for post-mating behavioral changes.

Circadian control of courtship across a 24-h period

One reason for *fru* to be expressed in the core clock is to regulate the time of day when courtship occurs. Previous reports indicated that courtship peaks during the night, in assays that used automated tools to measure behavior.[36,37] Male courtship behavior of flies with activated, silenced, and control *fru* ∩ *Clk* neurons was recorded for 24 h in 12-h light and 12-h dark conditions, on the third day after being loaded into the chambers with females, to allow recovery from being transferred and to examine courtship in a context when females will be less receptive. The 24 h of video footage were manually coded for courtship behavior at evenly spaced intervals. We find across all three genotypes that males court similarly (Figures 6A and 6B). We see an increase in courtship ~2 h before lights-on, with the peak in courtship behavior at lights-on across all three genotypes (Figures 6C–6E). We do see that when *fru* ∩ *Clk* neurons are activated or silenced there is a trend to seeing more courtship during the day (Figure 6). One possible explanation for the difference in these results and the previous report regarding when courtship peaks[36] is that we find automated coding of videos overestimates the time males spend courting because the automated programs score flies being in close proximity to females as courting[38] (Figure S14).

DISCUSSION

We show that the *fru* ∩ *Clk* neurons direct sex-specific changes in circadian period length and impact male courtship behavior. The fact that both activating and silencing the *fru* ∩ *Clk* neurons results in a shorter period length in males suggests that activity modulation in these neurons is important for maintenance of the circadian period. We found that males have more *fru* ∩ *Clk* DN3 neurons, which may account for the stronger male circadian phenotype. An examination of the *fru* ∩ *Clk* neurons from our connectome annotations and a more focused analysis on the functions of *fru* ∩ *Clk* subsets will help address the basis for the sex difference. Our identification of additional Gal4 transgenes that subset the *fru* ∩ *Clk* neurons can be used to understand the roles of smaller populations of neurons. Although a lot is known about the clock, this study provides additional annotation of the DN3 clock neurons, which is a class that is not well understood compared to other clock neurons. Why the circadian period length in males is more sensitive to changes in *fru* ∩ *Clk* neuronal activity and which neurons direct this difference is an interesting next question. Additionally, it will be important to understand if there are additional behavioral outputs these neurons could impact in different behavioral paradigms. Our labeling of fru^{+} post-synaptic targets of the clock also show additional sexual dimorphism downstream of the clock that is important to understand.

We found a link between the clock and courtship, with activation of *fru* ∩ *Clk* neurons changing the rate of copulation attempts. Other studies have linked circadian regulatory neurons to mating behavior[39–44] and the clock Pdf neuropeptide to sex differences in activity patterns.[45] This suggests a role for *fru* ∩ *Clk* neurons in courtship gating or timing. Developing higher resolution tools to automate the quantification of courtship behavior will address if the molecular clock resides in the *fru* circuit to direct the timing of courtship across the day. Our lower powered, manual scoring of 16 males per genotype indicates that courtship activity peaks around lights-on, demonstrating a link between the clock and courtship. Increasing the power of the analyses by scoring the courtship of 50–100 animals across a 24-h period will likely yield additional roles for *fru* ∩ *Clk* neurons, as this is the typical number used to reveal other circadian phenotypes. Overall, this study provides an additional model to understand how neural networks that have a role in distinct behaviors can cross-influence behavioral outcomes with co-expression of the master regulatory transcription factors providing strong inroads to address the question.

Limitations of the study

The *fru* ∩ *Clk* neurons investigated in this study are defined by a set of molecular genetic tools. Therefore, this is not an all-encompassing analysis of neurons that express *fru P1* and circadian transcription factors. Indeed, additional populations were identified using additional molecular genetic tools (Figures S3–S5). In addition, this study relies on a large set of Flp-out transgenic tools, so an additional limitation is that we do not know if the "stop cassettes" are similarly removed from each of the transgenes. We also note that higher resolution analyses of the confocal data, using methodologies like Sholl analysis, might reveal additional sex differences in morphology of the *fru* ∩ *Clk* neurons. Finally, we were not able to test all the neuropeptides that are known to be released from the circadian clock neurons, given we were not able to obtain antibodies.

RESOURCE AVAILABILITY

Lead contact

Requests for further information and resources should be directed to and will be fulfilled by the lead contact, Michelle Arbeitman (michelle.arbeitman@med.fsu.edu).

Materials availability

- This study did not generate new unique reagents.
- All stable reagents generated in this study are available from the lead contact without restriction.

Data and code availability

- Original data generated in this paper will be shared by the lead contact upon request.
- There is no original code generated for the results reported in this manuscript.
- Any additional information needed to reanalyze the data reported in this paper will be available from the lead contact.

ACKNOWLEDGMENTS

We thank the Bloomington Drosophila Stock Center (NIH P40OD018537) and Drosophila colleagues for generously providing stocks and antibodies. Several antibodies used in this study were obtained from the Developmental Studies Hybridoma Bank, created by the NICHD of the NIH and maintained at The University of Iowa, Department of Biology, Iowa City, IA 52242. We used FlyBase to find information about genes, stocks, phenotypes, and function.[46] We thank Adela Peña and Jackson Mast for their contributions to some of the experiments presented. We also thank Colleen Palmateer for R code and helpful input. The co-first authors are listed alphabetically, by first name. We thank the two anonymous reviewers for their helpful comments. In the graphical abstract we used a brain template copied from Biorender (Arbeitman has a license). This work was supported by NIH MIRA grant 5R35GM145282 and NIH R01GM073039 and R01GM116998.

AUTHOR CONTRIBUTIONS

Investigation, A.D., B.B., D.K.P., M.A.K., M.T., and M.N.A.; formal analysis, A.D., B.B., D.K.P., M.A.K., M.T., and M.N.A; conceptualization, M.N.A.; writing—original draft, A.D., B.B., and M.A.K.; writing—review & editing, A.D., B.B., M.A.K., M.T., and M.N.A.; visualization, A.D., B.B., D.K.P., and M.A.K.; supervision, M.N.A.; project administration, M.N.A.; funding acquisition, M.N.A.

DECLARATION OF INTERESTS

The authors declare no competing interests. D.K.P. is now affiliated with Center for Precision Medicine, Wake Forest University School of Medicine, Winston-Salem, North Carolina, USA. M.T. is now affiliated with Programs in Biomedical Sciences, University of Miami Miller School of Medicine, Miami, Florida, USA.

STAR★METHODS

Detailed methods are provided in the online version of this paper and include the following:

- KEY RESOURCES TABLE
- EXPERIMENTAL MODEL AND STUDY PARTICIPANT DETAILS
  - Drosophila husbandry and genetic strains

SUPPLEMENTAL INFORMATION

Supplemental information can be found online at https://doi.org/10.1016/j.isci.2025.112037.

Received: June 16, 2024
Revised: December 16, 2024
Accepted: February 12, 2025
Published: February 15, 2025

REFERENCES

1. Dubowy, C., and Sehgal, A. (2017). Circadian Rhythms and Sleep in Drosophila melanogaster. Genetics *205*, 1373–1397. https://doi.org/10.1534/genetics.115.185157.
2. Asahina, K. (2018). Sex differences in Drosophila behavior: Qualitative and Quantitative Dimorphism. Curr. Opin. Physiol. *6*, 35–45. https://doi.org/10.1016/j.cophys.2018.04.004.
3. Palmateer, C.M., Artikis, C., Brovero, S.G., Friedman, B., Gresham, A., and Arbeitman, M.N. (2023). Single-cell transcriptome profiles of Drosophila fruitless-expressing neurons from both sexes. Elife *12*, e78511. https://doi.org/10.7554/eLife.78511.
4. Cavanaugh, D.J., Vigderman, A.S., Dean, T., Garbe, D.S., and Sehgal, A. (2016). The Drosophila Circadian Clock Gates Sleep through Time-of-Day Dependent Modulation of Sleep-Promoting Neurons. Sleep *39*, 345–356. https://doi.org/10.5665/sleep.5442.
5. Guo, F., Yu, J., Jung, H.J., Abruzzi, K.C., Luo, W., Griffith, L.C., and Rosbash, M. (2016). Circadian neuron feedback controls the Drosophila sleep–activity profile. Nature *536*, 292–297. https://doi.org/10.1038/nature19097.
6. Schlichting, M., Richhariya, S., Herndon, N., Ma, D., Xin, J., Lenh, W., Abruzzi, K., and Rosbash, M. (2022). Dopamine and GPCR-mediated modulation of DN1 clock neurons gates the circadian timing of sleep. Proc. Natl. Acad. Sci. USA *119*, e2206066119. https://doi.org/10.1073/pnas.2206066119.
7. Zhang, Y., Liu, Y., Bilodeau-Wentworth, D., Hardin, P.E., and Emery, P. (2010). Light and temperature control the contribution of specific DN1 neurons to Drosophila circadian behavior. Curr. Biol. *20*, 600–605. https://doi.org/10.1016/j.cub.2010.02.044.
8. Sun, L., Jiang, R.H., Ye, W.J., Rosbash, M., and Guo, F. (2022). Recurrent circadian circuitry regulates central brain activity to maintain sleep. Neuron *110*, 2139–2154.e5. https://doi.org/10.1016/j.neuron.2022.04.010.
9. Sato, K., and Yamamoto, D. (2023). Molecular and cellular origins of behavioral sex differences: a tiny little fly tells a lot. Front. Mol. Neurosci. *16*, 1284367. https://doi.org/10.3389/fnmol.2023.1284367.
10. Stockinger, P., Kvitsiani, D., Rotkopf, S., Tirián, L., and Dickson, B.J. (2005). Neural circuitry that governsmale courtship behavior. Cell *121*, 795–807. https://doi.org/10.1016/j.cell.2005.04.026.
11. Manoli, D.S., Foss, M., Villella, A., Taylor, B.J., Hall, J.C., and Baker, B.S. (2005). Male-specific fruitless specifies the neural substrates of Drosophila courtship behaviour. Nature *436*, 395–400. https://doi.org/10.1038/nature03859.
12. Auer, T.O., and Benton, R. (2016). Sexual circuitry in Drosophila. Curr. Opin. Neurobiol. *38*, 18–26. https://doi.org/10.1016/j.conb.2016.01.004.
13. Yu, J.Y., Kanai, M.I., Demir, E., Jefferis, G.S.X.E., and Dickson, B.J. (2010). Cellular organization of the neural circuit that drives Drosophila courtship behavior. Curr. Biol. *20*, 1602–1614. https://doi.org/10.1016/j.cub.2010.08.025.
14. Gummadova, J.O., Coutts, G.A., and Glossop, N.R.J. (2009). Analysis of the Drosophila Clock promoter reveals heterogeneity in expression between subgroups of central oscillator cells and identifies a novel enhancer region. J. Biol. Rhythms *24*, 353–367. https://doi.org/10.1177/0748730409343890.
15. Talay, M., Richman, E.B., Snell, N.J., Hartmann, G.G., Fisher, J.D., Sorkaç, A., Santoyo, J.F., Chou-Freed, C., Nair, N., Johnson, M., et al. (2017). Transsynaptic Mapping of Second-Order Taste Neurons in Flies by trans-Tango. Neuron *96*, 783–795.e4. https://doi.org/10.1016/j.neuron.2017.10.011.
16. Nern, A., Pfeiffer, B.D., and Rubin, G.M. (2015). Optimized tools for multicolor stochastic labeling reveal diverse stereotyped cell arrangements in the fly visual system. Proc. Natl. Acad. Sci. USA *112*, E2967–E2976. https://doi.org/10.1073/pnas.1506763112.
17. Fernandez, M.P., Berni, J., and Ceriani, M.F. (2008). Circadian remodeling of neuronal circuits involved in rhythmic behavior. PLoS Biol. *6*, e69. https://doi.org/10.1371/journal.pbio.0060069.
18. Reinhard, N., Fukuda, A., Manoli, G., Derksen, E., Saito, A., Möller, G., Sekiguchi, M., Rieger, D., Helfrich-Förster, C., Yoshii, T., and Zandawala, M. (2024). Synaptic connectome of the Drosophila circadian clock. Nat. Commun. *15*, 10392. https://doi.org/10.1038/s41467-024-54694-0.
19. Blau, J., and Young, M.W. (1999). Cycling vrille expression is required for a functional Drosophila clock. Cell *99*, 661–671. https://doi.org/10.1016/s0092-8674(00)81554-8.
20. Stoleru, D., Peng, Y., Nawathean, P., and Rosbash, M. (2005). A resetting signal between Drosophila pacemakers synchronizes morning and evening activity. Nature *438*, 238–242. https://doi.org/10.1038/nature04192.
21. Deng, B., Li, Q., Liu, X., Cao, Y., Li, B., Qian, Y., Xu, R., Mao, R., Zhou, E., Zhang, W., et al. (2019). Chemoconnectomics: Mapping Chemical Transmission in Drosophila. Neuron *101*, 876–893.e4. https://doi.org/10.1016/j.neuron.2019.01.045.
22. Sekiguchi, M., Inoue, K., Yang, T., Luo, D.G., and Yoshii, T. (2020). A Catalog of GAL4 Drivers for Labeling and Manipulating Circadian Clock Neurons in Drosophila melanogaster. J. Biol. Rhythms *35*, 207–213. https://doi.org/10.1177/0748730419895154.
23. Diaz, M.M., Schlichting, M., Abruzzi, K.C., Long, X., and Rosbash, M. (2019). Allatostatin-C/AstC-R2 Is a Novel Pathway to Modulate the Circadian Activity Pattern in Drosophila. Curr. Biol. *29*, 13–22.e13. https://doi.org/10.1016/j.cub.2018.11.005.
24. Meiselman, M.R., Alpert, M.H., Cui, X., Shea, J., Gregg, I., Gallio, M., and Yapici, N. (2022). Recovery from cold-induced reproductive dormancy is regulated by temperature-dependent AstC signaling. Curr. Biol. *32*, 1362–1375.e8. https://doi.org/10.1016/j.cub.2022.01.061.
25. Dorkenwald, S., McKellar, C.E., Macrina, T., Kemnitz, N., Lee, K., Lu, R., Wu, J., Popovych, S., Mitchell, E., Nehoran, B., et al. (2022). FlyWire: online community for whole-brain connectomics. Nat. Methods *19*, 119–128. https://doi.org/10.1038/s41592-021-01330-0.
26. Schlegel, P., Yin, Y., Bates, A.S., Dorkenwald, S., Eichler, K., Brooks, P., Han, D.S., Gkantia, M., Dos Santos, M., Munnelly, E.J., et al. (2024). Whole-brain annotation and multi-connectome cell typing of Drosophila. Nature *634*, 139–152. https://doi.org/10.1038/s41586-024-07686-5.
27. Ryner, L.C., Goodwin, S.F., Castrillon, D.H., Anand, A., Villella, A., Baker, B.S., Hall, J.C., Taylor, B.J., and Wasserman, S.A. (1996). Control of male sexual behavior and sexual orientation in Drosophila by the fruitless gene. Cell *87*, 1079–1089. https://doi.org/10.1016/s0092-8674(00)81802-4.
28. Dalton, J.E., Fear, J.M., Knott, S., Baker, B.S., McIntyre, L.M., and Arbeitman, M.N. (2013). Male-specific Fruitless isoforms have different regulatory roles conferred by distinct zinc finger DNA binding domains. BMC Genom. *14*, 659. https://doi.org/10.1186/1471-2164-14-659.

29. Neville, M.C., Nojima, T., Ashley, E., Parker, D.J., Walker, J., Southall, T., Van de Sande, B., Marques, A.C., Fischer, B., Brand, A.H., et al. (2014). Male-specific fruitless isoforms target neurodevelopmental genes to specify a sexually dimorphic nervous system. Curr. Biol. *24*, 229–241. https://doi.org/10.1016/j.cub.2013.11.035.

30. von Philipsborn, A.C., Jörchel, S., Tirian, L., Demir, E., Morita, T., Stern, D.L., and Dickson, B.J. (2014). Cellular and behavioral functions of fruitless isoforms in Drosophila courtship. Curr. Biol. *24*, 242–251. https://doi.org/10.1016/j.cub.2013.12.015.

31. Anand, A., Villella, A., Ryner, L.C., Carlo, T., Goodwin, S.F., Song, H.J., Gailey, D.A., Morales, A., Hall, J.C., Baker, B.S., and Taylor, B.J. (2001). Molecular genetic dissection of the sex-specific and vital functions of the Drosophila melanogaster sex determination gene fruitless. Genetics *158*, 1569–1595. https://doi.org/10.1093/genetics/158.4.1569.

32. Cichewicz, K., and Hirsh, J. (2018). ShinyR-DAM: a program analyzing Drosophila activity, sleep and circadian rhythms. Commun. Biol. *1*, 25. https://doi.org/10.1038/s42003-018-0031-9.

33. Simpson, J.H. (2016). Rationally subdividing the fly nervous system with versatile expression reagents. J. Neurogenet. *30*, 185–194. https://doi.org/10.1080/01677063.2016.1248761.

34. Wohl, M., Ishii, K., and Asahina, K. (2020). Layered roles of fruitless isoforms in specification and function of male aggression-promoting neurons in Drosophila. Elife *9*, e52702. https://doi.org/10.7554/eLife.52702.

35. Kwon, Y., Kim, S.H., Ronderos, D.S., Lee, Y., Akitake, B., Woodward, O.M., Guggino, W.B., Smith, D.P., and Montell, C. (2010). TRPA1 Channel Is Required to Avoid the Naturally Occurring Insect Repellent Citronellal. Curr. Biol. *20*, 1672–1678. https://doi.org/10.1016/j.cub.2010.08.016.

36. Fujii, S., Krishnan, P., Hardin, P., and Amrein, H. (2007). Nocturnal male sex drive in Drosophila. Curr. Biol. *17*, 244–251. https://doi.org/10.1016/j.cub.2006.11.049.

37. Fujii, S., and Amrein, H. (2010). Ventral lateral and DN1 clock neurons mediate distinct properties of male sex drive rhythm in Drosophila. Proc. Natl. Acad. Sci. USA *107*, 10590–10595. https://doi.org/10.1073/pnas.0912457107.

38. Chiara, V., and Kim, S.Y. (2023). AnimalTA: A highly flexible and easy-to-use program for tracking and analysing animal movement in different environments. Methods Ecol. Evol. *14*, 1699–1707. https://doi.org/10.1111/2041-210x.14115.

39. Kadener, S., Villella, A., Kula, E., Palm, K., Pyza, E., Botas, J., Hall, J.C., and Rosbash, M. (2006). Neurotoxic protein expression reveals connections between the circadian clock and mating behavior in Drosophila. P Natl. Acad. Sci. USA *103*, 13537–13542. https://doi.org/10.1073/pnas.0605962103.

40. Levine, J.D., Funes, P., Dowse, H.B., and Hall, J.C. (2002). Resetting the circadian clock by social experience in. Science *298*, 2010–2012. https://doi.org/10.1126/science.1076008.

41. Sakai, T., and Ishida, N. (2001). Circadian rhythms of female mating activity governed by clock genes in Drosophila. Proc. Natl. Acad. Sci. USA *98*, 9221–9225. https://doi.org/10.1073/pnas.151443298.

42. Krupp, J.J., Kent, C., Billeter, J.C., Azanchi, R., So, A.K.C., Schonfeld, J.A., Smith, B.P., Lucas, C., and Levine, J.D. (2008). Social experience modifies pheromone expression and mating behavior in male Drosophila melanogaster. Curr. Biol. *18*, 1373–1383. https://doi.org/10.1016/j.cub.2008.07.089.

43. Hanafusa, S., Kawaguchi, T., Umezaki, Y., Tomioka, K., and Yoshii, T. (2013). Sexual interactions influence the molecular oscillations in DN1 pacemaker neurons in Drosophila melanogaster. PLoS One *8*, e84495. https://doi.org/10.1371/journal.pone.0084495.

44. Fujii, S., Emery, P., and Amrein, H. (2017). SIK3-HDAC4 signaling regulates Drosophila circadian male sex drive rhythm via modulating the DN1 clock neurons. Proc. Natl. Acad. Sci. USA *114*, E6669–E6677. https://doi.org/10.1073/pnas.1620483114.

45. Iyer, A.R., Scholz-Carlson, E., Bell, E., Biondi, G., Richhariya, S., and Fernandez, M.P. (2024). Sexually Dimorphic Influence of Circadian Pacemaker Neurons on Behavioral Rhythms. Preprint at bioRxiv. https://doi.org/10.1101/2024.01.31.578273.

46. Ozturk-Colak, A., Marygold, S.J., Antonazzo, G., Attrill, H., Goutte-Gattat, D., Jenkins, V.K., Matthews, B.B., Millburn, G., Dos Santos, G., Tabone, C.J., and FlyBase, C. (2024). FlyBase: updates to the Drosophila genes and genomes database. Genetics *227*, iyad211. https://doi.org/10.1093/genetics/iyad211.

47. Schneider, C.A., Rasband, and Eliceiri, K.W. (2012). NIH Image to ImageJ: 25 years of image analysis. Nat. Methods *9*, 671–675.

48. Sanders, L.E., and Arbeitman, M.N. (2008). Doublesex establishes sexual dimorphism in the Drosophila central nervous system in an isoform-dependent manner by directing cell number. Dev. Biol. *320*, 378–390. https://doi.org/10.1016/j.ydbio.2008.05.543.

STAR★METHODS

KEY RESOURCES TABLE

REAGENT or RESOURCE	SOURCE	IDENTIFIER
Antibodies		
Rabbit polyclonal α-Per	Rosbash Lab	N/A
Rat polyclonal α-FruM	Sanders and Arbeitman, 2008	N/A
Mouse monoclonal α-flag-tag	Sigma	Cat #: F1804 RRID: AB_262044
Rabbit monoclonal α-HA-tag	Cell Signaling	Cat #: 3724S RRID: AB_1549585
Chicken polyclonal α-myc-tag	Invitrogen	Cat #: A21281 RRID: AB_2535826
Rabbit polyclonal α-myc-tag	Abcam	Cat #: AB9106 RRID: AB_307014
Rabbit polyclonal α B-galactasidase	Thermo Fisher Scientific	Cat #: A11132 RRID: AB_221539
Rat monoclonal α-mouse CD8	Invitrogen	Cat#: 14008182 RRID: AB_467087
Mouse monoclonal α bruchpilot	DSHB	Cat #: nc82 RRID: AB_2318466
Mouse monoclonal α-PDF	DSHB	Cat #: PDF C7 RRID: AB_760350
Rabbit α-GFP Alexa Fluor 488	Invitrogen	Cat #: A21311 RRID: AB_221477
Goat α-rat Alexa Fluor 488	Invitrogen	Cat #: A11006 RRID: AB_2534074
Chicken α V5 polyclonal 550 conjugated	Novus Biologicals	Cat # NB600-379R RRID: AB_3194853
Rabbit α-V5 tag polyclonal 549 conjugated	Rockland	Cat #: 600-442-378 RRID: AB_1961802
Goat α-rabbit Alexa Fluor 633	Invitrogen	Cat #: A21071 RRID: AB_2535732
Goat α-mouse Alexa Fluor 488	Invitrogen	Cat #: A11001 RRID: AB_2534069
Goat α-mouse Alexa Fluor 633	Invitrogen	Cat #: A21052 RRID: AB_2535719
Goat α-rabbit Alexa Fluor 488	Invitrogen	Cat #: A32731 RRID: AB_2633280
Goat α-chicken Alexa Fluor 546	Invitrogen	Cat #: A11040 RRID: AB_2534097
Goat α-rat Alexa Fluor 568	Invitrogen	Cat #: A11077 RRID: AB_2534121
Experimental models: Organisms/strains		
D. melanogaster: w[*]; P{w[+mC]=Clk-GAL4.-856}2	Bloomington Stock Center	RRID: BDSC_93198
D. melanogaster: w[*]; P{y[+t*] w[+mC]=UAS(FRT.stop)TrpA1[myc]}VIE-260B	Bloomington Stock Center	RRID: BDSC_66871
D. melanogaster: w[*]; TI{FLP}fru[FLP]/TM3, Sb[1]	Bloomington Stock Center	RRID: BDSC_66870
D. melanogaster: w[*]; P{w[+mC]=UAS(FRT.stop)Hsap\KCNJ2}VIE-19A/CyO	Bloomington Stock Center	RRID: BDSC_67686
D. melanogaster: y[1] w[*] P{y[+t7.7] w[+mC]=5xQUAS-nlsDsRedT4}su(Hw)attP8; P{y[+t7.7] w[+mC]=trans-Tango}attP40/SM6b	Bloomington Stock Center	RRID: BDSC_95315
D. melanogaster: w[*]; P{y[+t7.7] w[+mC]=trans-Tango}attP40/CyO; P{y[+t7.7] w[+mC]=10XUAS-IVS-myr::tdTomato}attP2, P{w[+mC]=QUAS(FRT.stop)mCD8-GFP.P}5/TM6B	Bloomington Stock Center	RRID: BDSC_77482
D. melanogaster: Df(3R)fru[4-40], fru[4-40]/TM6B, Tb[1]	Bloomington Stock Center	RRID: BDSC_66692
D. melanogaster: y[1] sc[*] v[1] sev[21]; P{y[+t7.7] v[+t1.8]=TRiP.HMS04334}attP40	Bloomington Stock Center	RRID: BDSC_56912
D. melanogaster: y[1] sc[*] v[1] sev[21]; P{y[+t7.7] v[+t1.8]=TRiP.HMC05531}attP40	Bloomington Stock Center	RRID: BDSC_64513
D. melanogaster: TI{GAL4}fru[GAL4.P1.D]/TM3, Sb[1]	Bloomington Stock Center	RRID: BDSC_66696
D. melanogaster: w[1118]; P{w[+mC]=UAS-tra.F}20J7	Bloomington Stock Center	RRID: BDSC_4590
D. melanogaster: Canton S +/+;+/+;+/+;+/+	Heberlein Lab	N/A
D. melanogaster: w[1118];;;	Well Genetics	N/A
D. melanogaster: w; UAS-FruMA7	Stephen Goodwin Lab	N/A
D. melanogaster: w; UAS-FruMB25	Stephen Goodwin Lab	N/A
D. melanogaster: w; UAS-FruMC1	Stephen Goodwin Lab	N/A

(*Continued on next page*)

Continued

REAGENT or RESOURCE	SOURCE	IDENTIFIER
D. melanogaster: w[1118]; PBac{y[+mDint2] w[+mC]=10xUAS(FRT.stop)myr::smGdP-HA}VK00005 P{y[+t7.7] w[+mC]=10xUAS(FRT.stop)myr::smGdP-V5-THS-10xUAS(FRT.stop)myr::smGdP-FLAG}su(Hw)attP1	Bloomington Stock Center	RRID: BDSC_64093
D. melanogaster: w; Tsh-GAL80	Julie Simpson Lab	N/A
D. melanogaster: w[1118]; P{y[+t7.7] w[+mC]=R67F03-p65.AD}attP40/CyO; MKRS/TM6B, Tb[1]	Bloomington Drosophila Stock Center	RRID: BDSC_70786
D. melanogaster: w[1118]; P{y[+t7.7] w[+mC]=R77H08-GAL4.DBD}attP2	Bloomington Drosophila Stock Center	RRID: BDSC_69630
D. melanogaster: TI{2A-GAL4}AstC[2A-GAL4]/CyO	Bloomington Drosophila Stock Center	RRID: BDSC_84595
D. melanogaster: w[*]; TI{2A-GAL4}Dh44[2A-GAL4]/TM3, Sb[1]	Bloomington Drosophila Stock Center	RRID: BDSC_84627
D. melanogaster: w[*]; TI{2A-GAL4}sNPF[2A-GAL4]/CyO	Bloomington Drosophila Stock Center	RRID: BDSC_84706
D. melanogaster: TI{2A-GAL4}AstA[2A-GAL4]	Bloomington Drosophila Stock Center	RRID: BDSC_84593
D. melanogaster: TI{2A-GAL4}CNMa[2A-GAL4]/TM3, Sb[1]	Bloomington Drosophila Stock Center	RRID: BDSC_84619
D. melanogaster: TI{2A-GAL4}Dh31[2A-AC.GAL4]/CyO	Bloomington Drosophila Stock Center	RRID: BDSC_84623
D. melanogaster: w[1118]; P{w[+mC]=UAS-tim-GAL4}2	Bloomington Drosophila Stock Center	RRID: BDSC_80941
D. melanogaster: w[*]; P{y[+t7.7] w[+mC]=UAS-Crtc.GFP}attP40/CyO; PBac{y[+mDint2] w[+mC]=UAS-mCD8.mCherry-T2A-lacZ.nls}VK00005/TM2	Bloomington Drosophila Stock Center	RRID: BDSC_99656
D. melanogaster: w[1118]; P{y[+t7.7] w[+mC]=10xUAS(FRT.stop)myr::smGdP-FLAG-THS-10xUAS(FRT.stop)myr::smGdP-cMyc}su(Hw)attP5	Bloomington Drosophila Stock Center	RRID: BDSC_62122
D. melanogaster: P{w[+mC]=cry-GAL4.Z}24, w[*]; P{w[+mC]=Pdf-GAL80.S}96A/CyO	Bloomington Drosophila Stock Center	RRID: BDSC_80940
Software and algorithms		
Image J	Schneider et al.[47]	https://imagej.nih.gov/ij/
ShinyR-DAM	Cichewicz and Hirsh,[32]	https://karolcichewicz.shinyapps.io/shinyr-dam/
ZEN Blue 3.6	Zeiss	www.zeiss.com
AnimalTA	Chiara and Kim,[38]	http://vchiara.eu/index.php/animalta/animalta-illustrations
Graphpad Prism version 10.0.0	Graphpad Inc.	www.graphpad.com
Other		
Drosophila Activity Monitor (DAM)	Trikinetics	https://trikinetics.com
LSM 900 Confocal Microscope	Zeiss	https://zeiss.com

EXPERIMENTAL MODEL AND STUDY PARTICIPANT DETAILS

The model system used in this study is Drosophila melanogaster.

Drosophila husbandry and genetic strains

All strains, unless otherwise indicated, are aged in humidified incubators at 25°C on a 12-hr light and 12-hr dark cycle. The laboratory Drosophila media composition is: 33 l H2O, 237 g agar, 825 g dried deactivated yeast, 1560 g cornmeal, 3300 g dextrose, 52.5 g Tegosept in 270 ml 95% ethanol and 60 ml propionic acid. To control for impacts of strain background on several of the behavioral

studies the following genes/transgenes were introgressed for five generations into a common w^{1118} genetic background obtained from Well Genetics (Taiwan): w^{+} (control), *UAS <stop <TraA1::myc*, and *UAS<stop<Kir2.1*. Virgin females from these strains were crossed to *Clk856-Gal4*; fru^{FLP} males to perform experiments on circadian period length and activity (Figures 4 and S7–S9) and courtship (Figures 5, 6, and S10–S12). All flies in these experiments had wild type eye color. All females used in this study are virgin, unless otherwise indicated.

METHOD DETAILS

Immunostaining and microscopy

Adult brains and VNCs were dissected and imaged as previously described.[3] Both primary and secondary antibodies were diluted in TNT (Tris-NaCL-Triton buffer; 0.1 M Tris–HCl, 0.3 M NaCl, 0.5% Triton X-100). All confocal microscopy was performed on a Zeiss LSM 900 system, with Zeiss Plan-Apochromat 20x/0.8 and 63x/1.4 objectives. The z-stack slice interval for all images was 1.0μm or 2.0μm. A 1 Airy Unit (AU) pinhole size was selected in Zeiss software (ZEN Blue 3.6) for each laser line: 488 nm: 38 μm; 555 nm: 34 μm; and 639 nm: 39 μm. All images were acquired in 16-bit grayscale space at 1024 × 1024 or 512 x 512 pixel resolution (0.19x or 0.39x Nyquist Sampling) with bidirectional scanning.

The primary antibodies are rabbit α-Per (1:500; gift from Michael Rosbash), Rat α-Fru^{M} (1:200),[48] Mouse α-flag (1:500; Sigma, F1804), Rabbit α-HA-tag (1:300; Cell Signaling, 3724S), Rabbit α-Myc-tag (1:1000; Abcam, ab9106),Chicken α-Myc (1:1000; Invitrogen, A21281), Mouse α-PDF (1:1000; DSHB, PDF C7), Rabbit α-beta-galactosidase (1:500; Thermofisher, A11132), Rat α-mouse-CD8 (1:100; Invitrogen, 14008182), Mouse α-bruchpilot (1:500; DSHB, nc82). The secondary antibodies are: Rabbit α-GFP 488 (for Tango with Flp-out; 1:500; Invitrogen, A21311), Goat α-rat 488 (for anti-Fru; 1:500; Invitrogen, A11006), Rabbit α-V5 tag 549 (for MCFO,1:500; Rockland, 600-442-378), Chicken α-V5 tag 550 (for MCFO, 1:500; Novus Biologicals, NB600-379R), Goat α-rabbit 633 (for MCFO, 1:500; Invitrogen, A21071), Goat α-mouse 488 (for MCFO,1:500; Invitrogen, A11001), Goat α-mouse 633 (for Flag, 1:500; Invitrogen, A21052), Goat α-rabbit 488 (for Per and Myc-tag and beta-galactosidase,1:500; Invitrogen, 32731), Goat α-chicken 546 (for myc, 1:500; Invitrogen, A11040), Goat α-mouse 633 (for Pdf, 1:500; Invitrogen, A21052), Goat α-Rat 568 (for mCD8, 1:500; Invitrogen A11077).

Quantification of neuron numbers

To quantify *fru* ∩ *Clk* MCFO neurons and the *trans*-Tango post-synaptic *fru* targets, confocal images were blinded, and cell bodies and morphological structures were scored independently by 2 or 3 people using Zeiss microscopy software ZEN Blue 3.6. To ensure consistency across individuals scoring, we performed statistical tests on averaged cell body counts across the independent observers. The results were consistent across averaged counts and within each observer's counts. Number of samples used for cell-counting data is reported in the results sections.

Circadian assays

Circadian assays were performed using Trikinetics DAM5H (15 beam) and DAM IV (single beam) *Drosophila* activity monitors (Trikinetics, Waltham, MA) and all data was collected in 1 minute bins using DAM System 311. Flies were collected Monday – Wednesday and loaded into 5x65mm glass tubes that contained our standard laboratory food. Tubes containing the flies were kept in a LD 12:12 humidified incubator until being loaded into activity monitor on Friday. The incubator was sealed with tin foil to prevent any light leaking in. The light:dark (LD) assay was conducted at 25°C on a 12-hr:12-hr LD cycle and beam cross activity was recorded in one min bins for 15 days. Incubator lights turned on at 9 am and off at 9 pm. This resulted in 13 days of data analyzed for all genotypes in the LD assay. In the dark:dark (DD) assay, flies were first entrained and aged at 25°C on a 12-hr:12-hr LD cycle for 5-7 days, allowing for 2 days of LD data for analysis. Next, we switched to a 12-hr:12-hr DD cycle for 12 days allowing for 11 days of data analyzed for DD conditions and circadian period (constant darkness for 12 days). Beam cross activity for the DD assay was recorded in 1-min bins. Data were analyzed using ShinyR-DAM for both assays, excluding the first and last day the flies were placed in the incubator. Dead flies were considered those with less than 50 beam cross events per day and were removed from the analyses. ShinyR-DAM analysis of sleep was only performed on LD assay data. ShinyR-DAM measures sleep events using a 5-min sliding window, where 5 min of inactivity is considered a sleep event. Circadian period analysis was performed in ShinyR-DAM using the DD assay data. The default ShinyR-DAM parameters were used as follows: Chi-Sq testing range of 18–30 hr, a Chi-Sq period testing resolution of 0.2, and a rhythmicity (circadian strength) threshold for filtering arhythmic individuals (Qp.act/Qp.sig) of 1.

Per time series

0-24 hour-old control and experimental flies were collected and individually housed on days 1-4. On day 3-4 they began entrainment in LD (12:12) at 25°C. After 6-9 days of entrainment, the flies were placed in DD for 7-8 days until dissection on day 7-8. Flies were 14-16 days old at dissection. For DD conditions, individually housed flies were wrapped in aluminum foil, placed in light-proof mylar bags, and kept in a dark incubator at 25°C for 7-8 days until dissection. Incubator LD entrainment times were varied while dissections were performed at the same time of day, resulting in different zeitgeber times at dissection. For each dissection, individual vials of 10-15 flies were removed from the light-proof bags, aluminum foil unwrapped, and flies were anesthetized on a CO_2 pad. Flies were euthanized and permeabilized in 100% ethanol for 2-10 seconds, washed in PBS, and fixed in 4% paraformaldehyde in PBS (PFA) for

15 minutes. Fly heads were decapitated during PFA incubation. Brains were then dissected and fixed for an additional 10 minutes in 4% PFA and processed using our standard immunohistochemistry protocol, as described previously. Brains were incubated overnight at 4°C in primary antibodies, then washed in TNT and incubated in secondary antibody for 4-6 hours at room temperature (18-22°C) with gentle rocking. Brains were scanned on the confocal microscope with 20x air and 63x oil immersion objectives.

Immunostaining quantification for per time series

Confocal settings were kept consistent across all scans. Confocal scans were captured in 16-bit grayscale space using a 63x oil immersion lens at 0.45x digital zoom with bidirectional scanning and 1um or 2um z-slices. Pixel resolution was 512x512 or 1024x1024 (0.19x or 0.39x Nyquist Sampling). Confocal scan files (.czi) were quantified in ImageJ (Fiji) using the Bio-Formats Importer plugin. Individual cells of circadian neuron populations were identified based on location, morphology, and intensity of the PDF, PER, and myc signals. Nuclear regions of interest (ROIs) were drawn manually on a single slice of the z-stack for each cell of interest (1 cell = 1 ROI = 1 slice). Average Per staining pixel intensity was measured from nuclear ROIs. Average background pixel intensity was manually drawn as a representative region surrounding the cell population. Normalized Values = (Nuclear Signal – Background)/Background. Within hemibrains, each cell of a population was measured against a single common background for that population. Representative images were processed and exported using ImageJ. Maximum intensity projections were generated of z-stacks for circadian neuron populations. ‘‘Auto’’ Brightness and Contrast settings were applied to each channel of maximum projections in ImageJ. Scale bars = 10um.

Courtship and mating assays

For male courtship assays, all male flies were collected within 0-6 hours post-eclosion and aged individually for 5-10 days in an incubator at 25°C on a 12-hr light/12-hr dark cycle. Female Canton S virgin flies were collected, and group housed in groups of ~10 in an incubator at 25°C on a 12-hr light/ 12-hr dark cycle for 5-10 days. The assays were performed using a 10mm 8-well courtship chamber set on a 25°C -temperature block between ZT5 to ZT8. Courtship activity was recorded for 10 minutes or until successful copulation (n=~30). Video recordings were analyzed blinded using Nodulus Observer XT software. Courtship Index and Wing Index were measured by dividing the time the experimental male fly spent doing each respective behavior toward the female by the total observation time. Attempted copulations per minute, successful copulations and latency to all courtship behaviors were also recorded per experimental male genotype. For male remating assays, males were placed in a mini-vial with one virgin Canton S at ZT5-8 and allowed to mate. Males that mated were immediately assayed with a new virgin in courtship chambers, as above.

For female mating assays all female flies were collected as virgins and aged in groups of ~10 in an incubator at 25°C on a 12-hr light/12-hr dark cycle for 5-10 days. The Canton S males were individually aged as above for courtship. Latency to successful copulation was measured in courtship chambers, as described for male mating. For female remating assays, virgins of the experimental genotypes were single housed in mini-vials, as were Canton S males, and aged for 5-10 days 25°C on a 12-hr light/12-hr dark cycle. At ZT0-2 males were added to the female vials and mating was observed.

GraphPad Prism was used to perform statistical analysis and determine statistical significance using nonparametric Kruskal-Wallis ANOVA test with Dunn’s post-hoc correction for courtship index, all latency data and all remating data. A one-way ANOVA with Tukey’s Multiple Comparisons was conducted on wing index and attempts per minute data from our initial mating assay. The $fru^{4\text{-}40}$ courtship data was analyzed in Prism using a Mann-Whitney U Test.

Courtship assay over 24-hours

Flies that were video recorded were maintained in 12-hours light/12-hours dark conditions for the entire experiment. 5–10-day old male (individually housed) and virgin females (group housed) flies were added to a 24-well dish with 2mL of 20mM sucrose, and 0.75% agarose food. On day 3, after being housed in the 24-well dish, flies were recorded for 24-hours. Recordings were conducted using a PointGrey GRAS-20s4C-C camera and a 720nM IR lens. Flies were placed above an IR illuminated surface, and temperature was maintained at 25 C. Camera settings: 1024x768 15 fps. Video was recorded using OBS.

For manual coding, videos were segmented into 1-hour batches. Manual coding of any male courtships behavior was done for six evenly spaced 90 second intervals, for each hour. For each 90 second interval, males were either scored as courting or not courting, based on visual observation.

To score the videos using automated tracking, the videos were added to the AnimalTA platform, backgrounds were automatically generated, and flies were tracked using background subtraction. Tracked data was interpolated to remove missing values. x/y positions of flies were analyzed using the AnimalTA software and courtship was defined as any period where the flies were within 5 mm of each other. Courtship Index is the % of time the flies were within 5 mm for each hour.

Post-mating locomotor assay

Males 0-6 hours post-eclosion and virgin females were collected and aged individually for 5-10 days in mini-vials in an incubator at 25°C on a 12-hr light: 12-hr dark cycle. Matings were done in mini-vials from ZT0-ZT2 with the males or females of the experimental genotype being mated to a Canton S female or male, respectively. Following mating, both mated and unmated flies of the experimental genotype were placed individually in circadian vials, without anesthesia. Circadian vials were put into a DAM system to monitor activity immediately after mating, under LD conditions. Activity counts were collected starting at ZT 3 for 13 hours. For

daytime sleep, activity of mated females was analyzed from ZT 3-12 on day 1. For nighttime sleep, activity of mated females was analyzed from ZT12-15 on day 1, using a 1-minute sliding window analysis in excel to find 5-minute windows of inactivity. ShinyR-DAM was used to analyze activity from ZT 3-15 on day 1.

QUANTIFICATION AND STATISTICAL ANALYSES

The software used for statistical analyses was GraphPad Prism. All details can be found in the figure legends and STAR Methods section, including statistical test used, exact value of *n*, values plotted, and dispersion metrics. All symbols and p-values are described in the figure legends. Further details (e.g. Mann-Whitney U, etc.) are available in Table S2.